| 発表者氏名 | 論文タイトル名 | 発表誌名 | 巻名 | ページ | 出版年 |
|---|---|---|---|---|---|
| 金倉　譲 | 細胞の増殖･分化･死の制御破綻によるがん化 | がん細胞の生物学 | | 64-81 | 2006 |
| 金倉　譲，江副幸子 | トランスレーショナルリサーチの今日と明日 | 新医療 | 33 | 109-112 | 2006 |
| 松村　到，金倉　譲 | 細胞周期制御 | 再生医療のための分子生物学 | | 17-35 | 2006 |
| 松村　到，金倉　譲 | 造血器腫瘍に対する分子標的療法 | 日本内科学会雑誌 | 95 | 147-53 | 2006 |
| 松村　到，金倉　譲 | IL-6の作用．1．造血系への作用 | 血液フロンティア | 16 | 19-25 | 2006 |
| 松村　到，金倉　譲 | その他の慢性骨髄増殖疾患とJAK2遺伝子異常 | 血液フロンティア | 16 | 35-43 | 2006 |
| 松村　到，金倉　譲 | シグナル伝達を標的とする治療：Ras阻害剤 | Mebio | 23 | 55-69 | 2006 |
| 松村　到，金倉　譲 | 細胞内シグナル伝達分子を標的にした分子標的療法 | 総合臨床 | 55 | 1609-15 | 2006 |
| 松村　到，金倉　譲 | 分子標的療法の真の治療標的 | 総合臨床 | 52 | 683-88 | 2006 |
| 松村　到，金倉　譲 | HOXB4による造血幹細胞制御 | 血液・腫瘍科 | 33(3) | 569-78 | 2006 |

| 発表者氏名 | 論文タイトル名 | 発表誌名 | 巻名 | ページ | 出版年 |
|---|---|---|---|---|---|
| 松村　到，金倉　譲 | エリスロポエチン及びその変異体の新たな臨床応用 | Annual Review 血液 2006 | | 56-63 | 2006 |
| 松村　到，金倉　譲 | 消化管悪性リンパ腫の分類と診断 | 医学のあゆみ 別冊 消化器疾患 | | 689-93 | 2006 |
| 江副幸子，金倉　譲 | 慢性骨髄性白血病の分子標的療 | 総合臨床 | 55 | 1659-65 | 2006 |
| 政家寛明，織谷健司，金倉　譲 | アディポネクチンの抗炎症作用 | 臨床免疫 | 45 | 603-06 | 2006 |
| 西村純一，金倉　譲 | 発作性夜間ヘモグロビン尿症 | 最新医学 | 61 | 413-19 | 2006 |

# Ⅵ.研究成果の刊行物・印刷物

EXPERIMENTAL CELL RESEARCH 313 (2007) 1008–1023

available at www.sciencedirect.com

ScienceDirect

www.elsevier.com/locate/yexcr

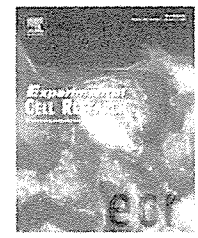

Research Article

# Isolation and characterization of bone marrow-derived mesenchymal progenitor cells with myogenic and neuronal properties

*Mitsutaka Shiota, Toshio Heike, Munetada Haruyama, Shiro Baba, Atsunori Tsuchiya, Hisanori Fujino, Hirohiko Kobayashi, Takeo Kato, Katsutsugu Umeda, Momoko Yoshimoto, Tatsutoshi Nakahata**

*Department of Pediatrics, Graduate School of Medicine, Kyoto University, 54 Kawahara-cho, Shogoin, Sakyo-ku, Kyoto 606-8507, Japan*

ARTICLE INFORMATION

*Article Chronology:*
Received 25 May 2006
Revised version received
21 November 2006
Accepted 27 December 2006
Available online 8 January 2007

*Keywords:*
Multipotent spheres
Murine bone marrow
Mesenchymal stem cells
Cardiomyocytes
Neurons
Skeletal myoblasts
Acute myocardial infarction

ABSTRACT

Sphere formation has been utilized as a way to isolate multipotent stem/progenitor cells from various tissues. However, very few studies on bone marrow-derived spheres have been published and assessed their multipotentiality. In this study, multipotent marrow cell populations were isolated using a three-step method. First, after elimination of hematopoietic cells, murine marrow-derived adherent cells were cultured in plastic dishes until small cells gradually appeared and multiplied. Cells were then cultured under non-adherent conditions and formed spheres that were immunopositive for a neural precursor marker, nestin. RT-PCR analysis also revealed that the spheres were positive for nestin in addition to PPARγ, osf2, SOX9, and myoD, which are markers of precursors of adipocytic, osteoblastic, chondrocytic, and skeletal myeloblastic lineages, respectively. Finally, spheres were dissociated into single cells and expanded in adherent cultures. Under appropriate induction conditions, the sphere-derived cells acquired the phenotypic properties in vitro of neurons, skeletal myoblasts, and beating cardiomyocytes, as well as adipocytes, osteoblasts, and chondrocytes. Next, sphere-derived cells were transplanted into murine myocardial infarction models. One month later, they had become engrafted as cardiomyocytes, and cardiac catheterization showed significant functional improvements. Thus, sphere-derived cells represent a new approach to enhance the multi-differentiation potential of murine bone marrow.



## Introduction

Human mesenchymal stem cells (MSCs), originally discovered by Friedenstein et al. [1] in 1976, can be isolated with relative ease from bone marrow utilizing plastic adherent methods [1,2]. MSCs can differentiate into three classical mesenchymal cell types (adipocytes, osteoblasts, and chondrocytes) [2]. Recently, they were also reported to be capable of differentiating into other lineages including neurons [3] and cardiomyocytes [4]. Based on this evidence, several clinical trials using human MSCs have been aimed at treating osteogenesis imperfecta [5], myocardial infarction [6], and so on. In addition, stem/progenitor cells with greater multipotentiality have been successfully isolated and expanded from human bone marrow

* *Corresponding author.* Fax: +81 75 752 2361.
E-mail address: tnakaha@kuhp.kyoto-u.ac.jp (T. Nakahata).

0014-4827/$ – see front matter © 2007 Elsevier Inc. All rights reserved.
doi:10.1016/j.yexcr.2006.12.017

stroma in the hope of developing treatments for a number of human diseases. These multipotent stem/progenitor cells include human marrow-isolated adult multi-lineage inducible (MIAMI) cells [7], multipotent adult progenitor cells (MAPCs) [8], and human BM-derived multipotent stem cells (hBMSCs) [9].

Several investigators have urged that cautions be exercised in therapeutic applications of such stem/progenitor cells until we have acquired a better understanding of their fundamental properties. Referring to MSCs, Javazon et al. [10] proposed that therapeutic trials with MSCs remain limited until the *in vivo* biology of MSCs and the therapeutic potential of passaged MSCs are better understood. For this purpose, *in vitro* and *in vivo* characterization of the biology of MSCs in non-human animals, such as mice, is necessary.

In contrast to human MSCs, easy and reproducible methods to enrich and expand murine MSCs have not yet been established. The isolation of murine MSCs by standard techniques involving adherence to plastic is difficult because of the possibility of contamination by macrophages, endothelial cells, lymphocytes, and smooth muscle cells both in early marrow populations and in passaged cultures [11]. Such unwanted cells often prevent the growth of MSCs. In addition, long-term *in vitro* culture of MSCs is difficult due to their tendency to lose progressively their capacity to proliferate and differentiate [10,12].

To overcome these problems, several groups have reported new protocols for isolating murine MSCs or marrow stem/progenitor cells. Most of the cells isolated, however, show differentiation potential into only two or three classical mesenchymal lineages [13–15]. The exception is murine MAPCs, which are difficult to isolate; many researchers including our own group, have failed to establish fully multipotent MAPCs. Therefore, it is necessary to establish more standardized culturing protocols for murine MSCs or marrow-derived multipotent stem/progenitor cells.

Sphere formation has been reported to constitute a step for the establishment of multipotent stem/progenitor cells from various tissues such as skin [16], mammary gland [17], and hepatocyte [18]. However, only a few studies identified bone marrow-derived spheres [3,19] that can differentiate into neurons and/or glial cells, and none of these reports addressed multipotentiality.

Here we report a method enabling isolation of murine bone marrow cells with greater multipotency than classical mesenchymal lineages. We assess the multi-differentiation potential in vitro of a cell population obtained by sphere formation, as well as their in vivo differentiation and functional capabilities in a model of acute myocardial infarction.

## Materials and methods

### *Isolation and culture of sphere-derived cells from murine bone marrow*

#### *Isolation*

Female 4- to 6-week-old C3H/He mice were purchased from Charles River Laboratories (Kyoto, Japan). All experiments in this study were performed in accordance with the Animal Protection Guidelines of Kyoto University. Bone marrow cells (BMCs) were obtained from five mice for each experiment as previously described [20]. Whole BMCs were suspended in Iscove's modified Dulbecco's medium (IMDM; Sigma, St. Louis, MO) supplemented with 20% heat-inactivated fetal calf serum (FCS; Gibco BRL, Grand Island, NY, Lot No: US172777), penicillin (100 IU/ml), and streptomycin (100 μg/ml) (complete medium).

To remove differentiated hematopoietic cells, lineage$^+$ cells were depleted from whole BMCs by means of immunomagnetic separation with Dynabeads according to the manufacturer's protocol. Briefly, BMCs were stained with primary rat-anti-mouse antibodies, namely anti-CD4, CD8, CD11b, CD45R/B220, Gr-1, and Ter119 (all purchased from PharMingen, San Jose, CA). After centrifugation of the labeled cells, Dynabeads M-450 Sheep anti-Rat IgG (Dynal Biotech, Oslo, Norway) were added at a concentration of 10 beads per cell. The mixture was placed on a Dynal Magnetic Particle Concentrator (Dynal Biotech) for one minute and the supernatant containing the lineage-depleted BMCs was collected.

Immunodepleted BMCs were resuspended in 10 ml of complete medium and plated on a 59-cm$^2$ Primaria™ tissue culture dish (BD Falcon, Lincoln Park, NY). Cells were cultured in a humidified incubator containing 5% $CO_2$ and 5% $O_2$ at 37 °C. After 24 h, non-adherent cells were removed by washing with phosphate-buffered saline (PBS) and fresh complete medium was added. Thereafter, the medium was changed twice a week for 3 to 4 weeks, when cells first reached 70–80% confluency. Then adherent cells were detached with Pronase (Kyokuto Seiyaku, Tokyo, Japan) for 30 min at 37 °C. Only easily detached cells were plated on a 59-cm$^2$ standard tissue culture dish (BD Falcon) (first passage). After the first passage, cells were cultured under similar conditions, except that the split ratio was set to 1:2. After an additional 5–7 passages, cells were detached at a lower cell density (40–50% confluence). The same conditions were used for subsequent cultures after small round and oval-shaped cells had become predominant at the sixth to eighth passage.

#### *Sphere formation and culture expansion*

A total of $1\times10^5$ cells were suspended in complete medium in each well of a 6-well ultra low attachment plate (Corning Inc., Corning, NY). Cells were cultured without changing the medium and rotated gently every 6 h. The spheres gradually increased in size and 7 days after suspension were picked and dissociated mechanically by gentle pipetting. Dissociated cells were cultured in complete medium on standard tissue culture dishes and the medium was changed twice a week. After reaching 40–50% confluency, cells were detached with Pronase and replated at a 1:4 dilution. Sphere-derived cells were harvested for the experiments described below when one well of the original culture contained more than $1\times10^7$ cells.

### *Flow cytometric analysis of sphere-derived cells*

Sphere-derived cells were analyzed by FACS Caliber (Becton Dickinson, San Jose, CA) as previously reported [21]. The following primary antibodies were used: fluorescein isothiocyanate (FITC)-conjugated CD29, CD49d, CD90.2 (Thy1.2), and H-2K$^k$ antibodies; phycoerythrin (PE)-conjugated Sca-1, CD13, CD31, CD34, CD49f, Flk-1, Gr-1, and Ter119 antibodies; (APC)-

conjugated CD45, CD45R/B220, and CD117 (c-kit) antibodies; biotinylated CD4, CD8a, CD11b/Mac1, CD44, CD144 (VE-cadherin), and I-$A^k$ antibodies; and purified rat anti-mouse CD105 antibody. In some experiments, streptavidin-FITC, PE, and APC conjugates and APC-conjugated goat anti-rat antibodies were used as secondary antibodies. Isotype control experiments were run in parallel using the same concentration of each antibody. All antibodies were purchased from PharMingen. At least 10,000 events were collected and analyzed with Cell Quest (BD Biosciences Clontech, Palo Alto, CA) software.

### *In vitro phenotypic acquisition of multiple lineages by sphere-derived cells*

*Adipogenic differentiation*

Adipogenic property was induced as previously described [2], except for the addition of 3-isobutyl-1-methylxanthine (IBMX). Briefly, confluent sphere-derived cells were cultured in α-minimum essential medium (α-MEM) supplemented with 10% FCS, 0.5 mM IBMX, 10 μg/ml insulin, and 1 μM dexamethasone (all from Sigma) for 21 days.

For Oil-red O staining, cells were fixed with 4% paraformaldehyde (PFA) and stained for 15 min in fresh Oil-Red O working solution (three volumes of 0.5% Oil Red O (Sigma) in isopropyl alcohol plus two volumes distilled water).

*Osteogenic differentiation*

To acquire the osteogenic property, confluent sphere-derived cells were cultured as described [2]. Briefly, cells were cultured in α-MEM with 10% FCS, 10 mM β-glycerophosphate, 50 μg/ml ascorbic acid 2-phosphate, and 10 nM dexamethasone (all from Sigma) for 28 days.

For alkaline phosphatase staining, cells were fixed with 4% PFA, washed in 10 mM Tris buffer (pH 7.5, Nakalai Tesque, Inc., Kyoto, Japan), and stained with alkaline phosphatase solution (5 mg naphthol AS-MX phosphate [Sigma] and 30 mg fast blue BB salt [Sigma] in 0.2 M Tris buffer [pH 8.5]) at room temperature (RT) for 30 min.

Mineralized matrix was evaluated by von Kossa staining. Cells were fixed with 4% PFA and overlaid with a 5% silver nitrate (Sigma) solution in the absence of light at RT for 30 min. Cells were then exposed to sunlight for 5 min and excess silver staining was removed by washing with a 5% sodium thiosulfate (Nakalai Tesque) solution.

*Chondrogenic differentiation*

The chondrogenic phenotype was acquired as previously described [22]. Briefly, confluent sphere-derived cells were cultured in Dulbecco's modified Eagles medium nutrient mixture F-12 HAM (Sigma) containing 5% FCS, 10 μg/ml transferrin, 10 μg/ml insulin, and $3\times10^{-8}$ M sodium selenite (all from Sigma) for 28 days.

For Alcian blue staining, the cells were fixed with methanol at −20 °C for 5 min and stained with 0.1% Alcian blue (0.1N HCl, Sigma) overnight.

*Neuronal differentiation*

To acquire the neuronal property, sphere-derived cells were treated as previously described [23] with some modifications. Briefly, cells were plated at a cell density of $1\times10^4$ cells/cm$^2$ on gelatin-coated dishes in neurobasal medium (Gibco BRL) with B27 Supplement (50×, Invitrogen, Carlsbad, CA), 20 ng/ml EGF (Sigma), and 10 ng/ml bFGF (Sigma) for 7 days, followed by culture in neurobasal medium with 0.5 μM retinoic acid (Sigma) and 20 ng/ml β-NGF (Sigma) for 5 days.

For immunofluorescence, cells were fixed in 4% PFA, permeabilized with 0.2% Triton X-100 in PBS at 4 °C for 30 min, blocked with 0.5% casein and 5% normal goat serum in PBS at 4 °C for 30 min, and sequentially incubated with anti-nestin (1:200; Chemicon International Inc., Temecula, CA) or β-tubulin III (1:500, Sigma) antibodies at 4 °C overnight, followed by incubation with secondary antibodies coupled with cytochrome 3 (Cy3, 1:200, Jackson Immunoresearch, West Grove, PA) at RT for 1 h. Between each step, cells were washed three times with 0.1% Tween in PBS. Fluorescence was detected and photographed with an AxioCam photomicroscope (Carl Zeiss Vision GmbH, Hallbergmoos, Germany). The immunofluorescent staining of a single sphere was performed as previously described [24].

*Skeletal myoblast and cardiomyocyte differentiation*

Skeletal myoblast and cardiomyocyte phenotypes were induced as described [4,25]. Briefly, confluent sphere-derived cells were first cultured in IMDM with 2% FCS and 0.5 μM 5-aza-2′-deoxycytidine (Sigma) for 24 h and then in IMDM with 10% FCS for 28 days.

Immunohistochemistry was performed as described [26]. Primary antibodies used in this study were anti-desmin (1:20 dilution, Sigma), skeletal myosin (1:50, Zymed Laboratories Inc., South San Francisco, CA), myosin light chain 2v (MLC2v, 1:100, Alexis Biochemicals Inc., Montreal, Canada) and atrial natriuretic peptide (ANP, 1:100; Protos Biotech, NY). Cells were stained with secondary antibodies coupled with horseradish peroxidase and reactions were visualized by adding 3, 3-diaminobenzidine (DAB, Vector Laboratories, Inc., Burlingame, CA).

*The percentage of phenotypically differentiated cells in each lineage*

After differentiation as described previously, the percentage of each phenotype was calculated in five randomly-selected fields (×200 magnification) by counting the number of nucleated cells by Hoechst33342 nuclear staining (1:2000, Molecular Probes, Leiden, The Netherlands) together with one of following stainings; Oil red O staining, alkaline phosphatase staining, Alcian blue staining, immunofluorescent staining for β-tubulin III, and DAB staining of skeletal myosin and MLC2v as described above. For cardiomyocytic differentiation, all the cardiomyocytes were counted in one 10-cm dish.

### *RNA isolation and RT-PCR analysis*

RT-PCR was undertaken as previously described [27] with the oligonucleotide primers listed in Table 1. For semi-quantitative comparisons, samples were normalized by dilution to yield equivalent signals for HPRT. Total RNAs from limb buds of murine embryos at 16.5 days post coitum (16.5 dpc) were used as positive controls for the chondrogenic lineage and those isolated at 18.5 dpc were used for adipogenic, osteogenic, and skeletal muscle lineages. Those

**Table 1 – Primers used for RT-PCR**

| Primer | Sequence | Product |
|---|---|---|
| Peroxisome proliferator activated receptor γ | S: 5′-ACCAAGTGACTCTGCTCAAG-3′<br>A: 5′-GGCTTCACGTTCAGCAAGCC-3′ | 279 bp |
| Adipocyte P2 | S: 5′-TGTGATGCCTTTGTGGGAACC-3′<br>A: 5′-CGTCTGCGGTGATTTCATCTG-3′ | 221 bp |
| Osteoblastic specific factor-2 | S: 5′-GAGGGCACAAGTTCTATCTGGAA-3′<br>A: 5′-CTACAACCTTGAAGGCCACG-3′ | 491 bp |
| Osteocalcin | S: 5′-TCTGACAAAGCCTTCATGTC-3′<br>A: 5′-AAATAGTGATACCGTAGATGCG-3′ | 201 bp |
| SOX9 | S: 5′-GAAGCTGGCAGACCAGTACC-3′<br>A: 5′-CTGCTCAGTTCACCGATGTC-3′ | 479 bp |
| Collagen type II | S: 5′-GTGAGCCATGATCCGC-3′<br>A: 5′-GACCAGGATTTCCAGG-3′ | 174 bp |
| Nestin | S: 5′-GGATACAGCTTTATTCAAGG-3′<br>A: 5′-CAGCCGCTGAAGTTCACTCT-3′ | 481 bp |
| Neurofilament M | S: 5′-CCTCTGTACACACACCGACA-3′<br>A: 5′-TAGCCTCAGGAGACTTCACG-3′ | 273 bp |
| MyoD | S: 5′-ATCCGCTACATCGAAGGTCT-3′<br>A: 5′-CTCTGGTGGTGCATCTGCCA-3′ | 371 bp |
| Myogenin | S: 5′-CAGTACATTGAGCGCCTACA-3′<br>A: 5′-ACATATCCTCCACCGTGATG-3′ | 264 bp |
| Desmin | S: 5′-ATCTCTGAGGCTGAAGAATGG-3′<br>A: 5′-GAGCAGAGAAGGTCTGGATAG-3′ | 414 bp |
| Myosin light chain 2v | S: 5′-GCCAAGAAGCGGATAGAAGG-3′<br>A: 5′-CTGTGGTTCAGGGCTCAGTC-3′ | 502 bp |
| Myosin light chain 2a | S: 5′-CAGACCTGAAGGAGACCT-3′<br>A: 5′-GTCAGCGTAAACAGTTGC-3′ | 278 bp |
| Nkx2.5 | S: 5′-CCAAGTGCTCTCCTGCTTTC-3′<br>A: 5′-GTAGCCATAGGCATTGAGAC-3′ | 503 bp |
| Oct-4 | S: 5′-GGCGTTCTCTTTGGAAAGGTG-3′<br>A: 5′-CTCGAACCACATCCTTCTCT-3′ | 315 bp |
| Rex1 | S: 5′-AAAGTGAGATTAGCCCCGAG-3′<br>A: 5′-TCCCATCCCCTTCAATAGCA-3′ | 933 bp |
| Brachyury | S: 5′-TTTCTTGGAAAAGCGGTGGC-3′<br>A: 5′-CCCGTTCACATATTTCCAGCG-3′ | 411 bp |
| HPRT | S: 5′-GCTGGTGAAAAGGACCTCT-3′<br>A: 5′-CACAGGACTAGAACACCTGC-3′ | 251 bp |

from whole brain of 18.5 dpc murine embryos and heart tissue from a 4-week-old mouse were used as positive controls for neuronal and cardiomyocytic lineages, respectively. Undifferentiated murine ES cells were used for Oct-4 and Rex1, and cells from 7.5 dpc mouse embryos were used for Brachyury.

### *Retroviral transduction of eGFP into sphere-derived cells*

Retroviral supernatants were produced by calcium phosphate-mediated transfection [28]. Briefly, phoenix cells, generously provided by Dr. G. Nolan, were transfected with a retroviral plasmid, pMSCV (murine stem cell virus)-EGFP (enhanced green fluorescent protein), which was kindly provided by Dr. R. Nishikomori, in DMEM/10%FCS for 8 h after which the medium was replaced. Two days after transfection, sphere-derived cells were incubated with the retroviral supernatant and 4 μg/ml polybrene (Sigma) and centrifuged at 1200×*g*, RT for 90 min. The supernatants containing the retrovirus were harvested after 20 h and the cells were incubated for another 2 days. Transduction efficiency was analyzed by FACS Caliber and $GFP^+$ cells were collected by cell sorting on FACS Vantage (Becton Dickinson).

### *In vivo engraftment of sphere-derived cells: acute myocardial infarction (AMI) model*

Male 10-week-old C3H/He mice were endotracheally intubated, anesthetized with 1% isoflurane gas, and ventilated by ventilators before ligating their left anterior descending coronary arteries. PBS (10 μl) containing $1\times10^6$ GFP-transduced sphere-derived cells, which were pretreated with 0.5 μM 5-aza-2′-deoxycytidine for 24 h, were directly injected with a 27-gauge needle into one site of the peri-infarcted area of the left ventricular free wall, and the chests were closed aseptically. Non-injected infarcted mice (AMI group) or infarcted mice injected with 10 μl PBS only (PBS group) and untreated normal mice served as controls (five mice for each group).

Four weeks after surgery, cardiac catheterization was performed to assess left ventricle (LV) function. Mice were anesthetized and their right carotid arteries were cannulated with 1.4-Fr micromanometer-tipped catheters (Millar Instruments Inc., Houston, TX) connected to pressure transducers (model TCB-500, Millar Instruments Inc.). Cardiac pressures were monitored and recorded on chart-strip recorders (Thermal Array Recorder, model RTA-1100M; Nihon Kohden, Tokyo, Japan). The maximum rate of LV

systolic pressure (+dP/dt), the minimum rate of LV diastolic pressure (−dP/dt), and LV end-diastolic pressure (LVEDP) were calculated from the inclination of the recorded pressure curves.

Subsequent immunohistochemistry was performed as described [26]. Implanted hearts were perfused with PBS and fixed with 4% PFA. After gradual equilibration in 15%, 20%, and 30% sucrose over 2 days, tissues were embedded in Optimal Cutting Temperature Compound (Ted Pella Inc., Redding, CA) and quickly frozen in liquid nitrogen. Cryostat sections (7 μm thick) were permeabilized and background staining due to endogenous murine immunoglobulins was eliminated using the Vector M.O.M. immunodetection kit (Vector Laboratories) according to the manufacturer's protocol. Sections were then stained with primary antibodies against cardiac troponin I (1:50, Santa Cruz Biotechnology Inc., Santa Cruz, CA), sarcomeric tropomyosin (1:100, Sigma), and CD31 (1:100, PharMingen) and were visualized with secondary antibodies conjugated to Cy3. For nuclear staining, cells were stained with Hoechst33342 at RT for one minute. Images were taken with fluorescent (Olympus, Tokyo, Japan) or confocal (Leica, Heerbrugg, Switzerland) stereomicroscopes. A total of 10 visual fields, where a cross section of capillaries was clearly visible, were randomly selected in the peri-infarct area, and the numbers of CD31-positive vessels were counted under ×200 magnification ($n=5$ per group).

### *Statistical analysis*

Results are presented as means±SD. Significant differences between two measurements were determined with the Student's *t*-test. *P* values <0.01 were considered significant.

## Results

### *Isolation of marrow-derived cells forming floating spheres*

Fig. 1 shows a schematic representation of the isolation of multipotent marrow cells using sphere formation. Cells grown in media containing the FCS had almost no ability to form hematopoietic colonies in the *in vitro* colony assays. To remove differentiated hematopoietic cells and prevent their excess growth, mature hematopoietic cells were depleted by immunomagnetic separation with Dynabeads. After depletion, the total number of cells was reduced from 4.2±0.85 (2.8 to 5.8, $n=5)\times10^8$ BMCs to 3.3±1.5 (1.0 to 5.7, $n=5)\times10^6$ BMCs. Since lineage$^-$ cells did not form symmetrical spheres in suspension cultures at this stage ($n=10$), we expanded them first in adherent cultures before sphere formation.

When lineage$^-$ cells were plated on standard tissue culture dishes, adherent cells did not proliferate to form colonies. Thus, we plated them on Primaria™ tissue culture dishes, which supported attachment and spreading of several cell types. After the medium was changed at 24 h, at most one adherent fibroblast-like cell per high-power field remained, and even on day 7, adherent cells appeared in the form of individual cells or clusters consisting of a few cells. However, adherent cells formed large heterogeneous colonies after 3–4 weeks when they were replated. After the first passage, adherent cells proliferated on standard tissue culture dishes, and after the sixth to eighth passage, small, round, and oval cells gradually increased and became predominant. Cells at this stage (non-spheres) were then cultured under their respective specialized differentiation conditions. In contrast to the three classical mesenchymal lineages, phenotypic

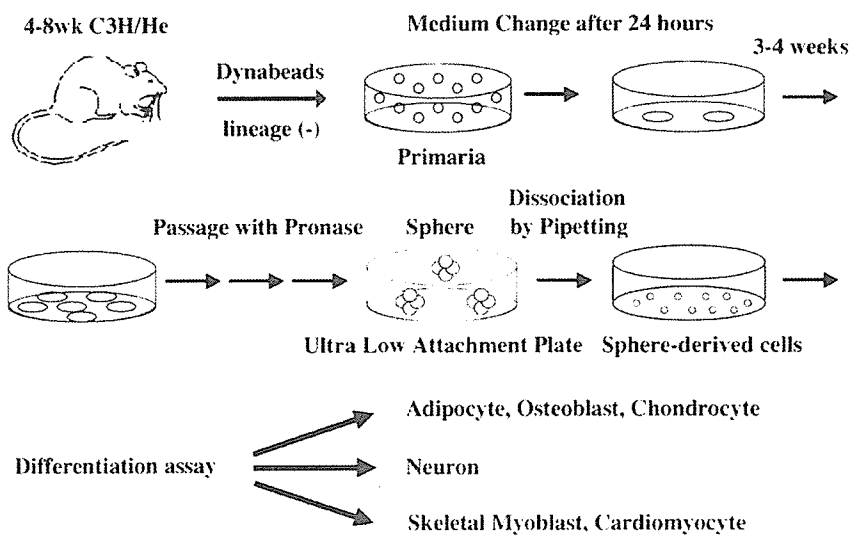


**Fig. 1 – Schematic representation of the protocol to generate multipotent marrow cell populations. Lineage$^-$ cells were selected from bone marrow cells of 4- to 6-week-old C3H/He mice using Dynabeads, plated on a Primaria™ tissue culture dish in IMDM supplemented with 20% FCS, and incubated in 5% $CO_2$ and 5% $O_2$. After 24 h, the medium was replaced and adherent cells were subcultured. After small, round to oval-shaped adherent cells had become predominant, cells were replated on an ultra low attachment plate, resulting in sphere formation. Spheres were collected and dissociated into single cells by gentle pipetting. Various methods were used to assess the differentiation potential of the sphere-derived cells both in vitro and in vivo.**

differentiation of other lineages was not seen (Table 2). During the acquisition of the neuronal phenotype, the cells changed their morphology to that of neuron-like cells (a small cell body with multiple long processes); however, the cells were negative for β-tubulin III and neurofilament M. During the induction of the skeletal myoblasts and cardiomyocytes, no morphological changes were observed and the cells were negative for skeletal myosin and MLC2v. Thus, we generated spheres to select for more primitive cells.

Approximately 3 months after the start of cultivation at a time when small round and oval-shaped cells predominated, adherent cells were capable of forming spheres on ultra low attachment plates. Many cells remained singular or formed small asymmetrical aggregates, but a few days after plating them in ultra low attachment plates, several small spherical clusters of floating cells appeared and thereafter these proliferated to generate larger symmetrical spheres (Fig. 2A). Initially, 13.1±4.2 spheres (range 5–15 spheres, $n=5$) were obtained from $5\times10^5$ adherent cells. Each sphere was composed of 375±63 cells (range 300–450 cells, $n=10$). Spheres were isolated, dissociated mechanically by gentle pipetting, and cultured again in fresh complete medium in standard tissue culture dishes. The shape of the sphere-derived cells was not homogeneous: cells were predominantly small (15–20 μm in diameter), round or oval-shaped (Fig. 2B), but medium-sized spindle- and star-shaped cells were also seen. No large flat fibroblastic cells were observed after dissociation of the spheres. Sphere-derived cells subsequently proliferated in adherent cultures, and adherent cells from a single sphere could generate multiple new spheres under non-adherent conditions.

### *Flow cytometry of sphere-derived cells*

For comparison with classic MSCs, we examined the surface epitopes of sphere-derived cells and found that they were strongly positive for Sca-1, CD13, CD29, CD44, CD49f, and CD105, weakly positive for CD34 and H-2K$^k$ (MHC class I) (Fig. 2C), and negative for all hematopoietic markers, namely, CD45 and Ter119 (Fig. 2C), and CD4, CD8, Gr-1, CD11b/Mac-1, CD45R/B220, and c-kit (data not shown). In addition, no expression of CD31, VE-cadherin, Flk-1, Thy1.2, and I-A$^k$ (MHC class II) was detected (data not shown). These cell surface profiles indicated that sphere-derived cells were phenotypically similar to classic MSCs [10] except for the expression patterns of CD34, c-kit, Flk-1, and Thy1.2.

**Table 2 – Adherent cells without passing through the sphere formation step were not induced into neuron-like cells, skeletal myoblasts, nor beating cardiomyocytes**

| Lineages | Assessments | Total trials | Positive results |
|---|---|---|---|
| Adipocytes | Oil-Red O staining | 5 | 5 |
| Osteoblasts | ALP staining | 5 | 5 |
| Chondrocytes | Alcian blue staining | 10 | 2 |
| Neurons | β-Tubulin III (Cy3) | 30 | 0 |
| | Neurofilament-M (RT-PCR) | | |
| Skeletal myoblasts | Skeletal myosin (DAB) | 30 | 0 |
| Cardiomyocytes | MLC2v (DAB) | 30 | 0 |

Each experiment was performed as described in material and methods. Without sphere formation, the adherent cells before sphere formation step could differentiate into adipocytes, osteoblasts, and chondrocytes, as assessed by Oil red O staining, alkaline phosphatase staining, and Alcian blue staining, respectively. In neuronal induction, they acquired the morphology of neuron-like cells but were immunonegative for β-tubulin III and did not express neurofilament-M in RT-PCR analysis. In skeletal myoblastic and cardiomyocytic differentiation, cells did not acquire characteristic morphology and were negative for DAB staining with skeletal myosin and MLC2v.

### *In vitro phenotypic acquisition of three classical mesenchymal lineages by sphere-derived cells*

To characterize sphere-derived cells, we first analyzed their differentiation potential into three classical mesenchymal cell types. One week after adipogenic induction, morphologic changes as well as formation of intracellular lipid vacuoles were noticeable. The vacuoles became larger by day 21 (Fig. 3A) as shown clearly by Oil-red O staining (Fig. 3B), and 23.6±6.8% of the cells were positive ($n=3$). RT-PCR showed expression of two adipocyte marker genes, peroxisome proliferator-activated receptor γ (PPARγ) and adipocyte P2 (aP2), in differentiated cells (Fig. 3C).

Acquisition of the osteoblastic property was followed by alkaline phosphatase staining (Fig. 3D), which showed that 12.6±3.7% of the cells were positive ($n=3$). Von Kossa staining showed the presence of a mineralized matrix (Fig. 3E). RT-PCR analysis confirmed the osteogenic property by showing an increase in the expression of osteoblastic-specific factor-2 (osf2) and induction of osteocalcin (OCN) in the differentiated cells (Fig. 3F).

Induction of the chondrogenic property resulted in acquisition of the characteristic morphology (Fig. 3G) [29] and sulfated proteoglycans as detected by Alcian blue staining (Fig. 3H), and 3.4±2.1% of the cells was positive ($n=3$). RT-PCR showed expression of SOX9 and collagen type II (col II) in differentiated cells (Fig. 3I).

Expressions of PPARγ, osf2, and SOX9 were already be detectable, although weakly, before adipogenic, osteogenic, and chondrogenic induction (Figs. 3C, F, I) respectively, and the expression of these markers increased after these inductions. On the other hand, expression of aP2, OCN, and col II could not be detected before the induction of each phenotype, but the cells tested positive for these markers after each induction. Five experiments were performed for each of these classical mesenchymal differentiations, and the same results were obtained in each experiment.

### *In vitro acquisition of the neuronal phenotype by sphere-derived cells*

We examined the differentiation capability of sphere-derived cells into lineages other than the three classical mesenchymal cell types. For investigation of the differentiation potential into the neuronal lineage, the cells were seeded at a low density and cultured in serum-free medium with EGF and bFGF, followed by stimulation with retinoic acid and NGF. After 12 days of differentiation, adherent cells acquired the morphology of neurons, displaying a cell body

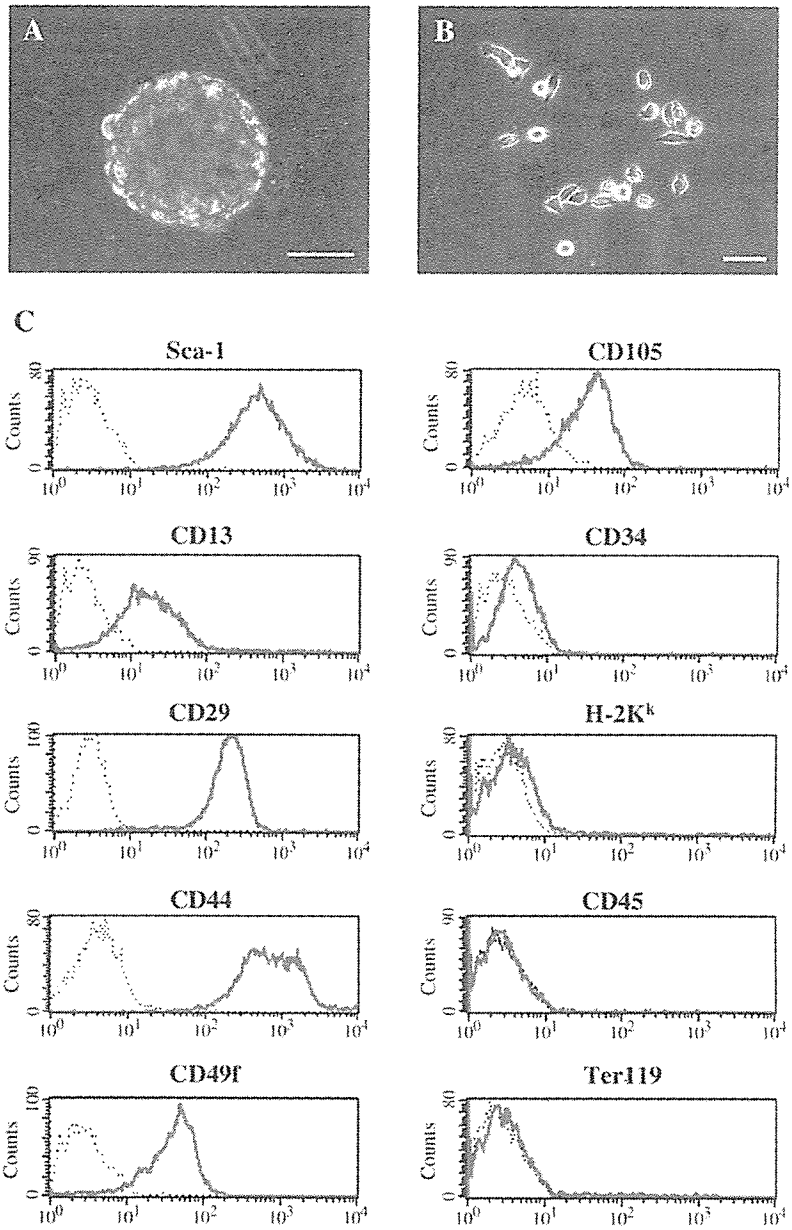


**Fig. 2 – Characteristics of isolated cells. Morphology of a sphere 7 days after suspension in ultra low attachment plates (A) and of adherent cells after sphere dissociation (B). All scale bars represent 50 μm. Sphere-derived cells were labeled with antibodies against CD13, CD29, CD34, CD44, CD45, CD49f, CD105, H-2K$^k$, Sca-1, and Ter119 and analyzed by flow cytometry (C). The dotted thin line indicates the isotype control IgG-staining profile and the thick line the antibody-staining profile. Representative results from one of three independent experiments are shown.**

with extended processes and a network-like structure in areas of higher cell density (Fig. 4A). Immunofluorescent assays on cells with phenotypic changes showed staining for nestin (Fig. 4B) and β-tubulin III (Fig. 4C) on day 12 of induction, and 51.2±28.3% of cells were positive for β-tubulin III ($n$=3), but negative for glial-fibrillary acidic protein (data not shown). RT-PCR analysis detected weak expression of nestin before induction and an increase in expression after neuronal induction (Fig. 4D). Expression of neurofilament M was detected only in cells displaying phenotypic changes (Fig. 4D).

Five experiments were performed for neuronal induction, and the same results were obtained in four of these. In one trial, neuron-like cells formed but could not be stained with β-tubulin III in the immunofluorescent assay and failed express neurofilament M as shown by RT-PCR analysis. In the other four experiments, these two assays yielded the same positive results.

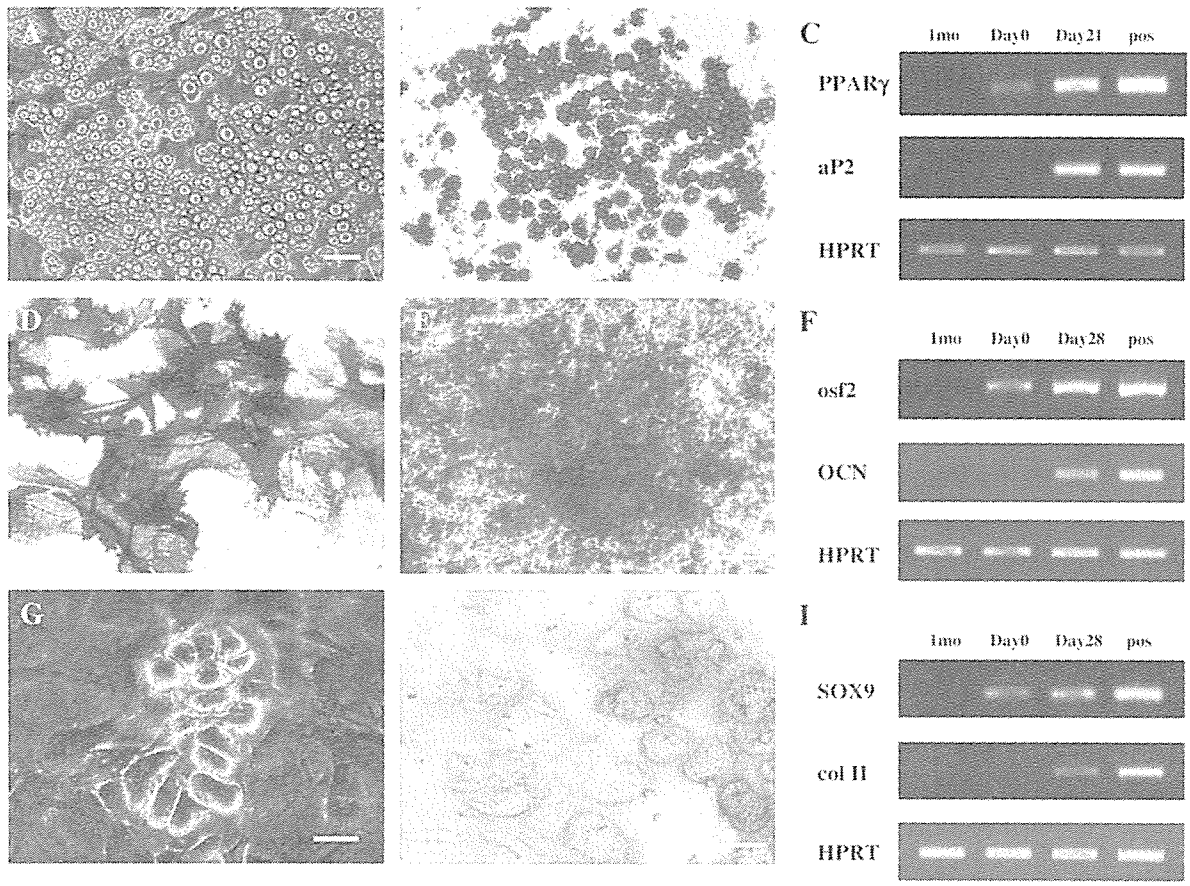


**Fig. 3 – Sphere-derived cells acquired phenotypic properties of adipocytes, osteoblasts, and chondrocytes. The adipogenic property was shown by the presence of intracellular lipid vacuoles (A), Oil red O staining (B) and the expression of adipocyte-specific genes (C) after 21 days of induction. The osteogenic property was demonstrated by alkaline phosphatase staining (D), von Kossa staining (E), and the expression of bone-specific genes after 4 weeks of induction (F). The chondrogenic property was demonstrated by the characteristic morphology (G), Alcian blue staining (H), and expression of chondrocyte-specific genes after 28 days of induction (I). All scale bars represent 50 μm. 1 mo: 1 month after starting cultivation; Day 0 and Day 28: before and 28 days after induction of differentiation; pos: positive control (C and F: limb buds of an 18.5-dpc murine embryo; I: limb buds of a 16.5-dpc murine embryo).**

### *In vitro phenotypic acquisition of skeletal myoblasts by sphere-derived cells*

Differentiation into skeletal myoblasts was induced *in vitro* by stimulating confluent sphere-derived cells with 5-aza-2′-deoxycytidine. After 14 days, round cells appeared and became elongated (Fig. 4E) to form multinucleated myotubes (Fig. 4F), which then fused together. They were positive for DAB staining of skeletal myosin (Fig. 4F) and desmin (Fig. 4G), and 0.013±0.0021% of cells was positive for myosin ($n=3$). RT-PCR analysis demonstrated that the skeletal myogenic marker genes, myoD and myogenin, were expressed in cells showing phenotypic changes (Fig. 4H). MyoD, but not myogenin, was expressed weakly even before skeletal myogenic induction (Fig. 4H). Five experiments were performed for the phenotypic acquisition of skeletal myoblasts and the same results were obtained in all five experiments.

### *In vitro phenotypic acquisition of cardiomyocytes by sphere-derived cells*

Cardiomyocytic differentiation was also induced in vitro by culturing confluent cells under the same conditions as for skeletal myoblasts. After a longer period, that is, after about 3 weeks, beating ball-like cells appeared (Fig. 4I), and these became connected and elongated to form beating myotubes on day 28 (Fig. 4J). The beating ball-like cells and myotubes were positive for DAB staining of MLC 2v (Fig. 4K) and 0.0043± 0.00086% of the cells were positive for MLC2v ($n=3$), but not for ANP (data not shown). RT-PCR analysis showed that the beating cells were positive for MLC2v and Nkx2.5 and negative for MLC2a (Fig. 4L). None of these markers were expressed before cardiomyogenic induction (Fig. 4L). These patterns demonstrated phenotypic acquisition of ventricular properties because MLC2v is specifically expressed in ventricular cells [30] whereas expression of MLC2a is restricted to the

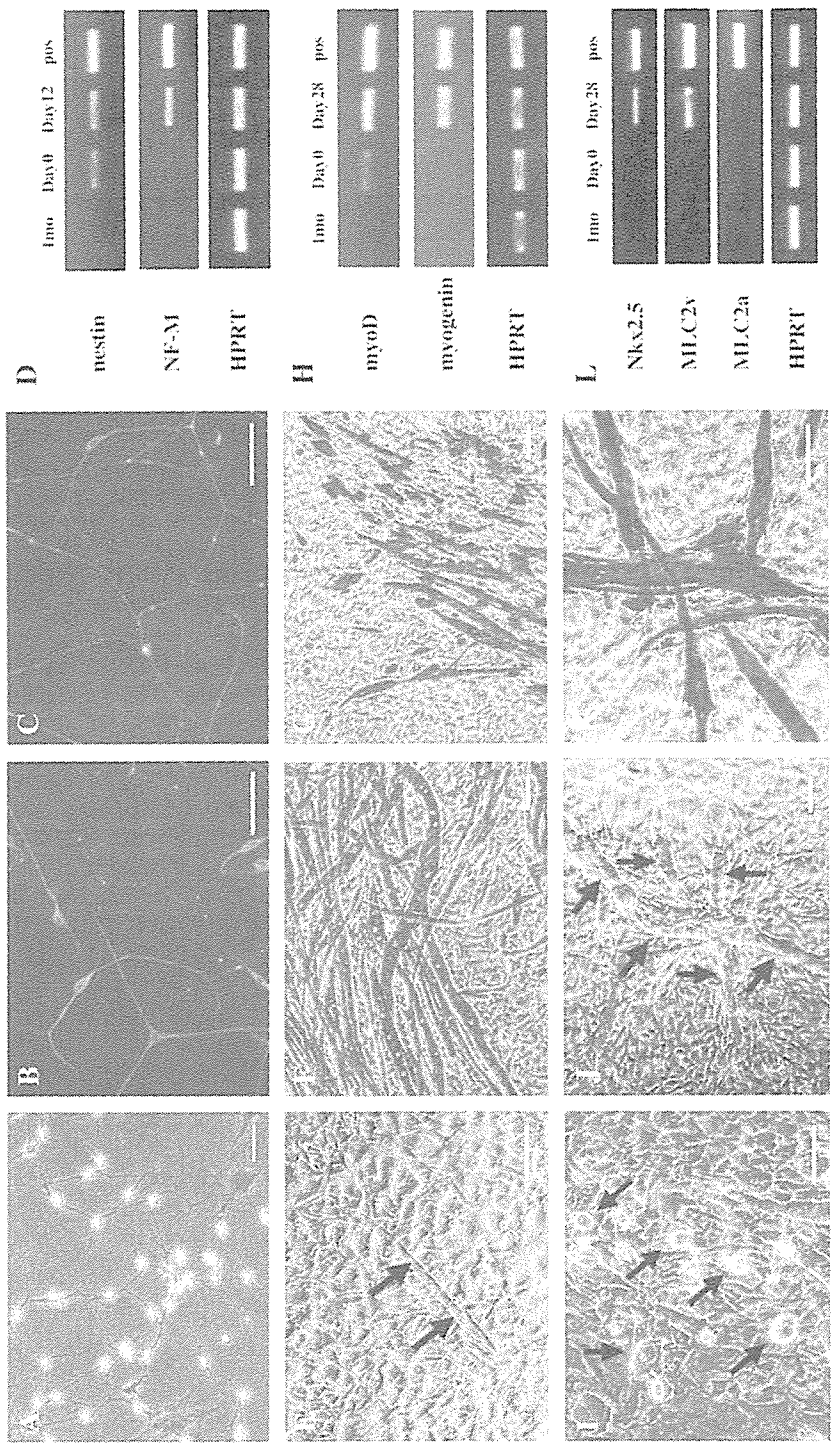


Fig. 4 – Sphere-derived cells acquired phenotypic properties of neurons, skeletal myoblasts, and cardiomyocytes. The neuronal property was demonstrated by the characteristic morphology and network structure after 12 days of induction (A), immuno-positivity for nestin (B) and β-tubulin III (C), and expression of appropriate markers (D). The skeletal myoblastic property was demonstrated by the formation of elongated multinucleated myotubes on day 14 (E, arrows) and day 28 (F, G) of induction, by DAB staining of skeletal myosin (F) and desmin (G), and by expression of skeletal muscle-specific genes (H). The cardiomyocytic property was evidenced by the appearance of beating round cells on day 21 (I, arrows) and beating myotubes on day 28 of induction (J, arrows; K), by DAB staining of MLC2v (K), and by expression of cardiomyocyte-specific genes (L). All scale bars represent 50 μm. 1 mo: 1 month after starting cultivation; Day 0, Day 12, and Day 28: before, 12 days after, and 28 days after induction of differentiation respectively; pos: positive control (D: whole brain of an 18.5-dpc murine embryo; H: limb buds of an 18.5-dpc murine embryo; L: whole heart of a 4-month-old mouse).

atrial myocardium [31]. Five experiments were performed for the acquisition of the cardiomyocytic phenotype, and the same results were obtained in four of these. In one experiment, no beating cardiomyocytes were obtained.

### *A single marrow-derived sphere expresses nestin and several mesodermal precursor markers and is composed of a heterogeneous cell population*

*In vitro* differentiation assays showed that sphere-derived cells could acquire the phenotypic properties of mesodermal (three classical mesenchymal cell types, skeletal myoblasts, and cardiomyocytes) and ectodermal (neurons) lineages. To determine whether a sphere expresses the markers of precursors of such lineages as well as other more primitive markers, we subjected a single sphere to RT-PCR analysis as shown in Fig. 5A. Spheres neither expressed undifferentiated ES cell markers, Oct-4 [32], or Rex1 [33], nor markers of the primitive mesoderm such as Brachyury [34] (Fig. 5A). However, a single sphere was positive for the neural precursor marker, nestin [40] (Fig. 5A). It also expressed transcription factor markers that are specific to the differentiation of three classical mesenchymal cells (PPARγ [35], osf2 [36], and SOX9 [37]) and skeletal myoblasts (myoD [38]) but did not express Nkx2.5 [39], a marker of cardiomyocyte differentiation (Fig. 5A).

In all cases, expression of these markers was maintained until induction of differentiation (Figs. 3C, F, I and 4D, H, L) and the sphere-derived cells showed multipotency as described above (Figs. 3A–B, D–E, G–H; Figs. 4A–C, E–G, I–K). Five experiments were performed, and each experiment gave similar results.

For a better understanding of the nature of spheres, we performed immunofluorescent analysis of a single sphere for nestin, which has been reported to be expressed in many multipotent spheres obtained from non-neural tissues [16,41,43]. As shown in Figs. 5B–E, most cells composing the sphere were weakly positive for nestin, but some cells located in the peripheral zone of a sphere expressed higher levels. This heterogeneous expression pattern was shared with other spheres ($n=22$). In contrast to spheres, adherent cells that had not undergone sphere formation were mostly nestin-negative, and only extremely weak expression was observed for a small portion of these cells ($1.8\pm0.54\%$, $n=3$, data not shown). These findings indicate that spheres neither correspond to a population of pluripotent ES cells nor to a primitive mesoderm, but rather constitute either a collection of multipotent progenitors of mesodermal and neural lineages at different differentiation stages, a diverse population of monopotent precursors, or a mixture of both.

To distinguish between these possibilities, we attempted single cell cloning of spheres by plating at a density of one cell per 2 wells of a 96-well plate and marking wells with single clones. In thirty 96-well plates, we identified several multipotent clones that were capable of acquiring the phenotypic properties of adipocytes, osteoblasts, chondrocytes, and skeletal myoblasts, in addition to monopotent clones of these lineages (data not shown). However, fully multipotent clone or monopotent clones of neurons or cardiomyocytes were not isolated. In theory, the multipotentiality of the spheres characterized here could be explained by the presence of a mixture of monopotent precursors of 6 cell types. However, if this were the case, all 6 cell types should have been obtained by single cell cloning, which was not the case.

To understand the role of the sphere-formation step, we performed RT-PCR analysis of all the markers examined in Fig. 5A and characterized the differences between spheres (Fig. 6, lane A), non-spheres, (Fig. 6, lane B), and the two clones obtained after single cell cloning (Fig. 6, lane C and D). Non-spheres did not express myoD, and compared to spheres, expressions of PPARγ, osf2, SOX9, and nestin were weaker (Fig. 6, lane B). These results indicated that spheres and non-spheres were composed of different cell populations. Judging from the results of the phenotypic differentiations shown in Table 2 and Figs. 3 and 4, spheres contained multipotent cell populations that were capable of generating more phenotypes than the cell population of non-spheres did. Clone 1 acquired the phenotypes of adipocytes, osteoblasts, and skeletal myoblasts and weakly expressed nestin in addition to precursor markers of each of these lineage (PPARγ, osf2, and myoD) (Fig. 6, lane C). Monopotent clone 2, which could differentiate into adipocytes, only expressed PPARγ (Fig. 6, lane C). These results indicated that the sphere-forming step favored for the acquisition of nestin-positivity and multipotency, which was impossible for the non-spheres in our method. In contrast, in single cell cloning, the expression of nestin regressed as clones lost their multipotency.

Therefore, we conclude that multipotent progenitors with the capacity to acquire phenotypic properties of neurons and/or cardiomyocytes as well as those of several mesenchymal cell lineages were generated by our method.

### *In vitro engraftment of sphere-derived cells as cardiomyocytes and functional improvement in the myocardial infarction model*

In order to determine if sphere-derived cells could repair damaged tissues, we first tagged them with eGFP, which showed that the efficacy of retroviral transduction ranged between 38% and 72% (Fig. 7A). After the $GFP^+$ cells had been sorted by FACS Vantage, sphere-derived cells were pretreated with 5-aza-2′-deoxycytidine and injected into the myocardium of an AMI model mouse.

Cardiac catheterization was performed 1 month later to determine whether transplantation of sphere-derived cells had a functional impact. LV systolic performance as assessed by LV +dP/dt in AMI (Fig. 7Bb) and PBS (Fig. 7Bc) groups decreased to 57.5% and 60.5% of that of normal control (Fig. 7Ba), respectively. Transplantation of $1\times10^6$ sphere-derived cells (Fig. 7Bd) resulted in a reduction of LV +dP/dt to 32.4% of that of normal control, which was a significant improvement compared with both PBS and AMI groups. The assessment of LV −dP/dt also showed a significant improvement in the cell-transplanted group compared with PBS and AMI groups (data not shown). Assessment of LV diastolic performance showed deterioration of LVEDP in all groups, but compared with PBS and AMI groups the LVEDP of cell-transplanted group was much better (Fig. 7C).

Immunofluorescent staining 28 days after surgery showed that $GFP^+$ cardiomyocytes were detected in all five experi-

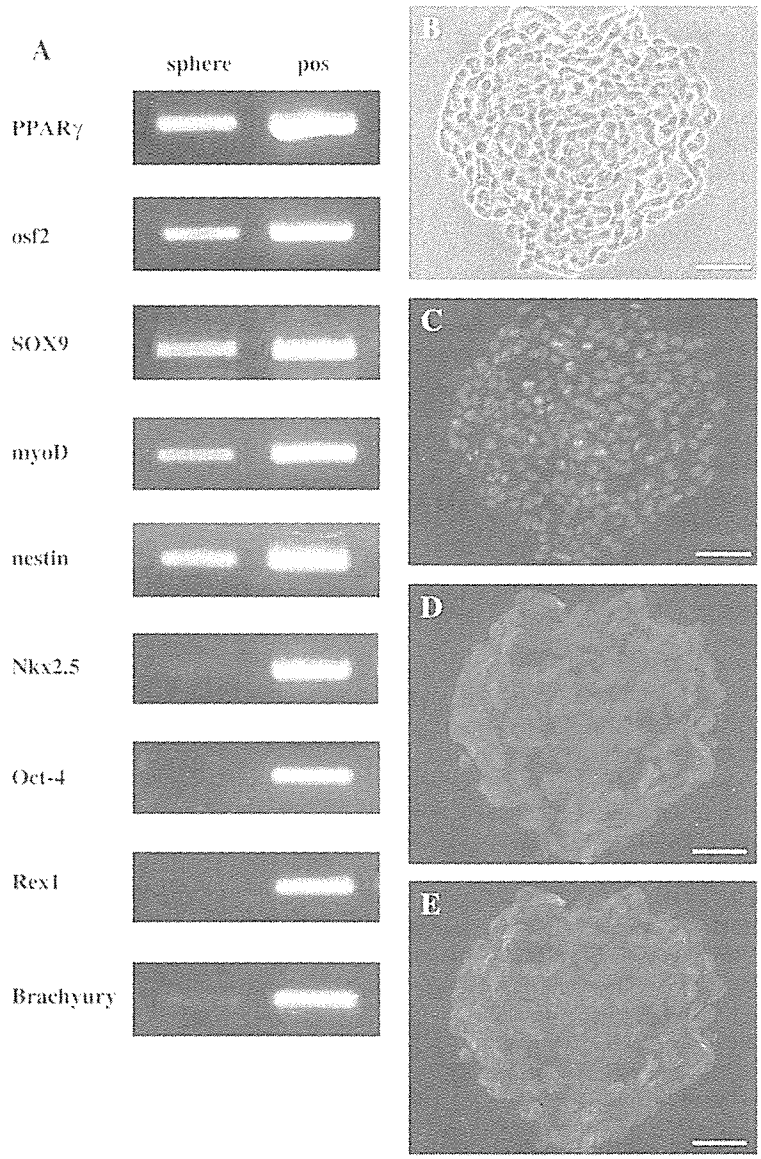


**Fig. 5 – Characteristics of a single sphere. (A) RT-PCR analysis of a sphere shows the transcription factors expressed during differentiation into three classical mesenchymal lineages (PPARγ, osf2, SOX9) and skeletal myoblasts (myoD), and the presence of a neural progenitor marker, nestin. The transcription factors of cardiomyocytes (Nkx2.5), undifferentiated ES cells (Oct-4, Rex1), and primitive mesoderm (Brachyury) were not expressed in the sphere. Sphere: a floating sphere 7 days after suspension in an ultra low attachment plate; pos: positive control (Oct-4 and Rex1: undifferentiated murine ES cells; Brachyury: murine embryo at 7.5 dpc; others: described in Figs. 3 and 4). (B–E) Immunofluorescent analysis of nestin in a sphere. The heterogenous expression patterns were similar with each other ($n$=22). All scale bars represent 50 μm. (B: bright field; C: Hoechst33352; D: nestin-Cy3; E: merged image).**

ments (see Figs. 7D–G for a representative experiment). GFP$^+$ cells were detectable in peri-infarction zones (Figs. 7D, E) and simultaneously expressed cardiac troponin I (Figs. 7F, G) and tropomyosin (data not shown). We searched for GFP positive cells from the apex to the base of the transplanted heart and found 6.8±2.6 ($n$=5) cells per heart. Considering the number of injected cells ($1\times10^6$ cells per mouse), the frequency of the cells engrafted as cardiomyocytes was very low (less than 0.001%).

Next, we evaluated angiogenesis by immunofluorescent analysis with CD31 (Fig. 7H). Increases in capillary numbers were observed at the peri-infarct zone in mice injected with sphere-derived cells. All CD31-positive cells were GFP-negative. Compared with PBS-injected (22.4±4.51 vessels) and AMI (25.4±7.30 vessels) groups, the cell-transplanted group (37.2±8.79 vessels) showed a marked increase ($0.01<p<0.05$) in CD31-positive vessels. No tumor formation was found in these experiments.

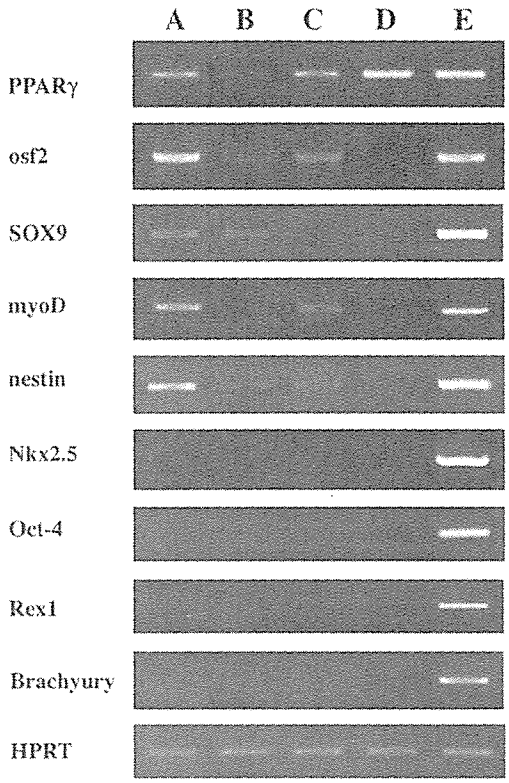


**Fig. 6 – RT-PCR analysis of spheres, non-spheres, and two clones. Spheres (A) showed different expression patterns of PPARγ, osf2, SOX9, myoD, and nestin, compared to non-spheres (B). Multipotent clone 1 (C) expressed the precursor markers of each lineage (PPARγ, osf2, myoD) and nestin weakly. Monopotent clone 2 (D) expressed only PPARγ. (A: floating spheres 7 days after suspension on an ultra low attachment plate; B: non-spheres; C: clone 1; D: clone 2; E: positive control as described in Fig. 5).**

These results showed that sphere-derived cells could be engrafted as cardiomyocytes only at low frequency *in vivo*, but stimulated host angiogenesis, and significantly improved cardiac function in the AMI model.

## Discussion

This study describes a method, based on sphere formation, which allows the isolation of a murine marrow-derived multipotent cell population that is capable of acquiring the phenotypic properties of adipocytes, osteoblasts, chondrocytes, neurons, skeletal myoblasts, and cardiomyocytes. The multipotent cell population also showed cardiomyogenic potential *in vivo* and had beneficial functional effects in an AMI model. To the best of our knowledge, this is the first evidence that multipotent spheres can be generated from bone marrow.

Without sphere formation, the culture conditions of adherent cells principally resembled those of MSCs that have been repeatedly shown to be pluripotential [3,10,25,42]. However, unlike MSCs, non-spheres in our method could not acquire phenotypes other than those of classical mesenchymal lineages. As the isolation of MSCs from murine bone marrow has been reported to be difficult [15], the conflicting results might be due to the differences in the isolation methods; strains of mice used (C3H/He) [15], starting cell populations (lineage negative marrow cells obtained with Dynabeads), and/or source of FCS (no check to support the growth of MSCs).

After forming spheres, cells acquired the phenotypic properties of multi-lineages. Immunofluorescent analysis showed that in contrast to most non-spheres, spheres expressed nestin, which was also confirmed by RT-PCR analysis, and were composed of a mixture of heterogeneous cell populations. Nestin has been reported in spheres of multipotent stem/progenitor cells of many non-neural tissues [16,41,43] and is suggested to be a marker of stem cells or an indicator of plasticity [41]. Moreover, only nestin-positive marrow stromal cells in rats were capable of forming spheres under specific culture conditions and differentiating into ectodermal lineage [47]. Therefore, spheres in our method might have acquired multipotency through enhanced expression of nestin.

Lots of recent reports on murine MSCs also showed immunopositivity for nestin [41,44,45], but its expression in MSCs seems to be still subject to some controversy [44]. The reported percentage of nestin-positive murine MSCs ranges widely from 3.1% to nearly 100%, whereas others have reported little expression [46]. Serum has been reported to inhibit nestin expression in rat marrow stromal cells [47], although most MSCs have been cultured in serum-rich medium and found to express nestin. These discrepancies could be also partially due to differences in isolation methods.

We suggested that our spheres could consist of four cell populations: multipotent stem/progenitor cells similar to those obtained from other tissue-derived multipotent spheres, multipotent precursors at different stages of differentiation, monopotent precursors of several lineages, or a mixture of these. To distinguish between these possibilities, we tried single cell cloning of a marrow-derived sphere, but could not isolate a multipotent clone capable of phenotypic acquisition of all 6 cell types or capable of producing monopotent clones of neurons or cardiomyocytes (data not shown). Several factors may account for our failure to establish fully multipotent clones. First, paracrine factors secreted by surrounding cells might be important for maintaining multipotentiality. Second, the acquired phenotypes of neurons and cardiomyocytes might be more easily lost when marrow stromal cells are used rather than other cell types. Third, we cannot exclude the possibility of technical problems. The frequency of fully multipotent progenitors might be small, which could have resulted in their loss during cloning. Alternatively, cell damage, greater than that after gentle pipetting, may have occurred when the pellets were dissociated vigorously into single cells at the time of cloning. In fact, we could not obtain a fully multipotent cell population when the spheres were dissociated by vigorous pipetting.

Despite these issues, our sphere-derived cells differ from classical murine MSCs and other marrow-derived stem/progenitor cells [2,13–15,48] as they displayed the phenotypic

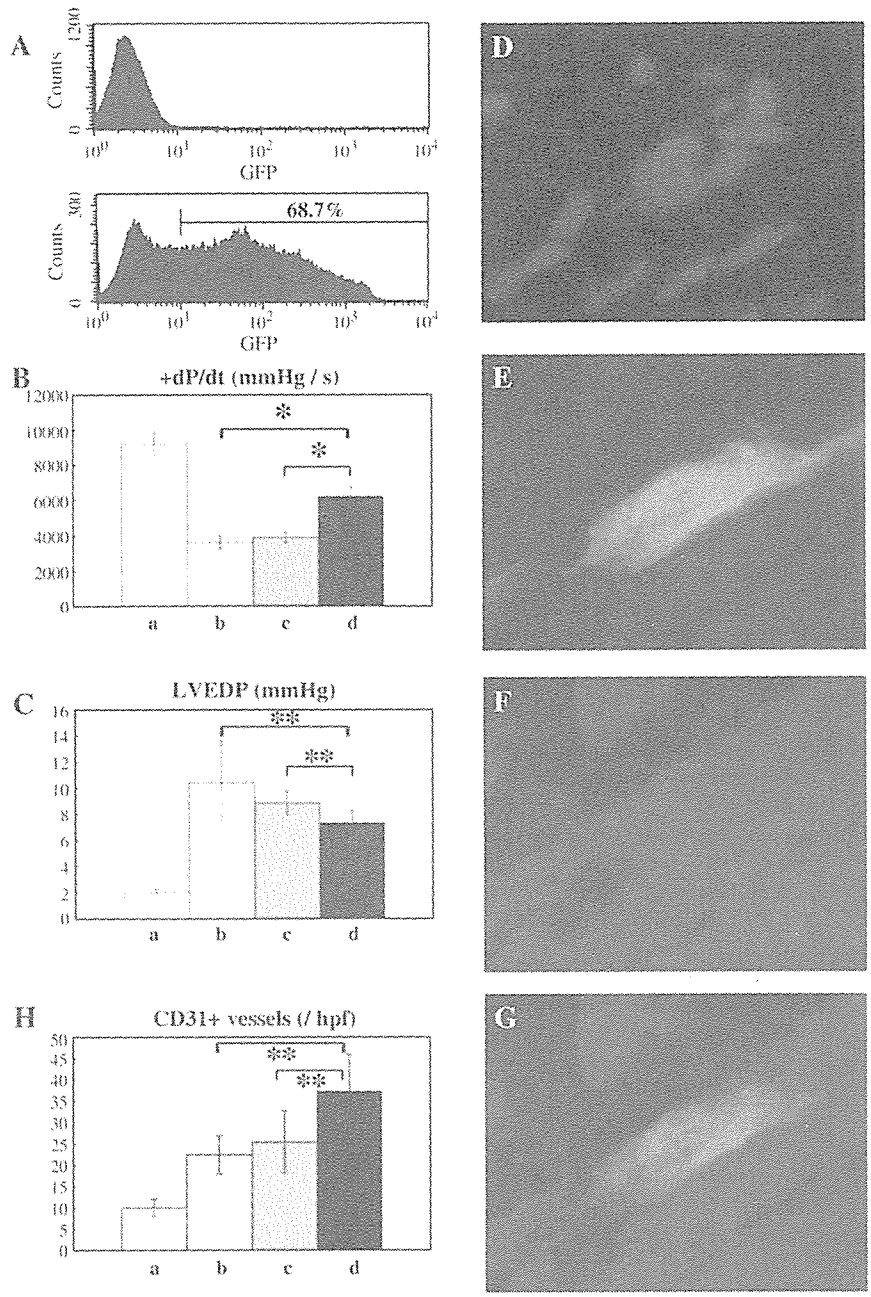


**Fig. 7 – Sphere-derived cells developed into cardiomyocytes and displayed improved cardiac function in a myocardial infarction model. Retroviral transduction of sphere-derived cells with GFP in FACS analysis (A). Upper and lower panels show untransduced and transduced cells, respectively. A total of $1\times10^6$ GFP-transduced cells were injected directly into a peri-infarcted area of infracted myocardium ($n=5$). Assessment of cardiac function with catheterization demonstrated significant improvement in +dP/dt (B) and LVEDP (C) compared with the non-injected infarcted-mice group and PBS-injected group, respectively (*$p<0.01$, **$0.01<p<0.05$, a: normal control; b: infarcted mice; c: infarcted mice injected with 10 μl PBS; d: infarcted mice injected with 10 μl PBS containing $1\times10^6$ GFP-transduced cells). Engraftment of implanted cells as cardiomyocytes was detected 28 days after surgery by immunofluorescence (D: Hoechst33342; E: GFP; F: troponin I-Cy3; G: merged image). Enhanced angiogenesis of CD31-positive and GFP-negative vessels was detected in the peri-infarct area of cell-injected mice compared to that in infracted-mice and PBS-injected mice (H, **$0.01<p<0.05$).**

characteristics of beating cardiomyocytes and acquired cardiomyogenic potential *in vivo*. Since Makino et al. [4] first reported the cardiomyogenic potential of murine bone marrow stromal cells (CMG cells), several researchers have shown differentiation of murine marrow-derived cells into cardiomyocytes in vitro and in vivo [49]. However, no group has

generated stem/progenitor cells or multipotent cell populations from bone marrow that can be subsequently induced to differentiate in vitro into beating cardiomyocytes. Like CMG cells, the sphere-derived cells underwent *in vitro* acquisition of the beating cardiomyocyte similar to CMG cells. This cardiomyogenic potential could be due to nuclear reprogramming by 5-aza-2′-deoxycytidine, a demethylating agent capable of altering gene expression [50]. Considering that no beating cardiomyocytes could be obtained under identical induction conditions without selection by sphere formation, the bone marrow-derived cells must have acquired cardiomyocytic potential during sphere formation.

Recently, CMG cells were found to be capable of differentiating into cardiomyocytes in vivo but no functional assessment of these cells was made [51]. BMCs [52] and MSCs [53] have also been reported to be capable of differentiating into cardiomyocytes in vivo. Although such cells improved cardiac function in AMI models in rat and swine, there has been little assessment of improved cardiac function in mice [49]. Our study is unique in that we performed catheterization in mice to undertake precise analysis of the effect of implanted cells on cardiac function. After transplantation into the heart of an AMI mouse, sphere-derived cells significantly improved cardiac function, although the engraftment frequency as cardiomyocytes was quite low. A similar outcome has been reported after transplantation of whole BMCs [54] or MSCs [55] in AMI models without engrafting as cardiomyocytes. Stimulation of host angiogenesis by donor cell-related factors has been reported as one of the reasons for the functional benefit [9,52,54]. Immunofluorescent analysis of CD 31 revealed enhanced host angiogenesis in cell-transplanted hearts, and this might partially contribute to the improved cardiac function in our model.

In summary, we present here a new method using sphere formation to isolate multipotent marrow progenitors in mice. After selection for sphere formation ability, cells showed multi-differentiation potential by crossing cell lineage boundaries *in vitro*. They also improved cardiac function when injected into an AMI model heart. When selection for sphere-forming ability was omitted, the cells lacked multipotentiality. These findings show that our three-step method based on sphere formation enhances the formation of multipotent progenitors from murine bone marrow.

## Acknowledgments

This study was supported by the Program for Promotion of Fundamental Studies in Health Science of the National Institute of Biomedical Innovation (NIBIO) (03-2) and Research of Japan, and by a Grant-in-Aid for Creative Scientific Research (13GS0009).

## REFERENCES

[1] A.J. Friedenstein, J.F. Gorskaja, N.N. Kulagina, Fibroblast precursors in normal and irradiated mouse hematopoietic organs, Exp. Hematol. 4 (1976) 267–274.
[2] M.F. Pittenger, A.M. Mackay, S.C. Beck, R.K. Jaiswal, R. Douglas, J.D. Mosca, M.A. Moorman, D.W. Simonetti, S. Craig, D.R. Marshak, Multilineage potential of adult human mesenchymal stem cells, Science 284 (1999) 143–147.
[3] A. Hermann, R. Gastl, S. Liebau, M.O. Popa, J. Fiedler, B.O. Boehm, M. Maisel, H. Lerche, J. Schwarz, R. Brenner, A. Storch, Efficient generation of neural stem cell-like cells from adult human bone marrow stromal cells, J. Cell Sci. 117 (2004) 4411–4422.
[4] S. Makino, K. Fukuda, S. Miyoshi, F. Konishi, H. Kodama, J. Pan, M. Sano, T. Takahashi, S. Hori, H. Abe, J. Hata, A. Umezawa, S. Ogawa, Cardiomyocytes can be generated from marrow stromal cells in vitro, J. Clin. Invest. 103 (1999) 697–705.
[5] E.M. Horwitz, D.J. Prockop, L.A. Fitzpatrick, W.W. Koo, P.L. Gordon, M. Neel, M. Sussman, P. Orchard, J.C. Marx, R.E. Pyeritz, M.K. Brenner, Transplantability and therapeutic effects of bone marrow-derived mesenchymal cells in children with osteogenesis imperfecta, Nat. Med. 5 (1999) 309–313.
[6] C. Stamm, B. Westphal, H.D. Kleine, M. Petzsch, C. Kittner, H. Klinge, C. Schumichen, C.A. Nienaber, M. Freund, G. Steinhoff, Autologous bone-marrow stem-cell transplantation for myocardial regeneration, Lancet 361 (2003) 45–46.
[7] G. D'Ippolito, S. Diabira, G.A. Howard, P. Menei, B.A. Roos, P.C. Schiller, Marrow-isolated adult multilineage inducible (MIAMI) cells, a unique population of postnatal young and old human cells with extensive expansion and differentiation potential, J. Cell Sci. 117 (2004) 2971–2981.
[8] M. Reyes, T. Lund, T. Lenvik, D. Aguiar, L. Koodie, C.M. Verfaillie, Purification and ex vivo expansion of postnatal human marrow mesodermal progenitor cells, Blood 98 (2001) 2615–2625.
[9] Y.S. Yoon, A. Wecker, L. Heyd, J.S. Park, T. Tkebuchava, K. Kusano, A. Hanley, H. Scadova, G. Qin, D.H. Cha, K.L. Johnson, R. Aikawa, T. Asahara, D.W. Losordo, Clonally expanded novel multipotent stem cells from human bone marrow regenerate myocardium after myocardial infarction, J. Clin. Invest. 115 (2005) 326–338.
[10] E.H. Javazon, K.J. Beggs, A.W. Flake, Mesenchymal stem cells: paradoxes of passaging, Exp. Hematol. 32 (2004) 414–425.
[11] P.L. Witte, M. Robinson, A. Henley, M.G. Low, D.L. Stiers, S. Perkins, R.A. Fleischman, P.W. Kincade, Relationships between B-lineage lymphocytes and stromal cells in long-term bone marrow cultures, Eur. J. Immunol. 17 (1987) 1473–1484.
[12] I. Sekiya, B.L. Larson, J.R. Smith, R. Pochampally, J.G. Cui, D.J. Prockop, Expansion of human adult stem cells from bone marrow stroma: conditions that maximize the yields of early progenitors and evaluate their quality, Stem. Cells 20 (2002) 530–541.
[13] S. Sun, Z. Guo, X. Xiao, B. Liu, X. Liu, P.H. Tang, N. Mao, Isolation of mouse marrow mesenchymal progenitors by a novel and reliable method, Stem. Cells 21 (2003) 527–535.
[14] P. Tropel, D. Noel, N. Platet, P. Legrand, A.L. Benabid, F. Berger, Isolation and characterisation of mesenchymal stem cells from adult mouse bone marrow, Exp. Cell Res. 295 (2004) 395–406.
[15] A. Peister, J.A. Mellad, B.L. Larson, B.M. Hall, L.F. Gibson, D.J. Prockop, Adult stem cells from bone marrow (MSCs) isolated from different strains of inbred mice vary in surface epitopes, rates of proliferation, and differentiation potential, Blood 103 (2004) 1662–1668.
[16] J.G. Toma, M. Akhavan, K.J. Fernandes, F. Barnabe-Heider, A. Sadikot, D.R. Kaplan, F.D. Miller, Isolation of multipotent adult stem cells from the dermis of mammalian skin, Nat. Cell Biol. 3 (2001) 778–784.
[17] G. Dontu, W.M. Abdallah, J.M. Foley, K.W. Jackson, M.F. Clarke, M.J. Kawamura, M.S. Wicha, In vitro propagation and

transcriptional profiling of human mammary stem/progenitor cells, Genes Dev. 17 (2003) 1253–1270.
[18] A. Tsuchiya, T. Heike, H. Fujino, M. Shiota, K. Umeda, M. Yoshimoto, Y. Matsuda, T. Ichida, Y. Aoyagi, T. Nakahata, Long-term extensive expansion of mouse hepatic stem/progenitor cells in a novel serum-free culture system, Gastroenterology 128 (2005) 2089–2104.
[19] Y. Torrente, M. Belicchi, F. Pisati, S.F. Pagano, F. Fortunato, M. Sironi, M.G. D'Angelo, E.A. Parati, G. Scarlato, N. Bresolin, Alternative sources of neurons and glia from somatic stem cells, Cell Transplant 11 (2002) 25–34.
[20] M. Yoshimoto, T. Shinohara, T. Heike, M. Shiota, M. Kanatsu-Shinohara, T. Nakahata, Direct visualization of transplanted hematopoietic cell reconstitution in intact mouse organs indicates the presence of a niche, Exp. Hematol. 31 (2003) 733–740.
[21] H. Hiramatsu, R. Nishikomori, T. Heike, M. Ito, K. Kobayashi, K. Katamura, T. Nakahata, Complete reconstitution of human lymphocytes from cord blood CD34+ cells using the NOD/SCID/gammacnull mice model, Blood 102 (2003) 873–880.
[22] C. Shukunami, C. Shigeno, T. Atsumi, K. Ishizeki, F. Suzuki, Y. Hiraki, Chondrogenic differentiation of clonal mouse embryonic cell line ATDC5 in vitro: differentiation-dependent gene expression of parathyroid hormone (PTH)/PTH-related peptide receptor, J. Cell Biol. 133 (1996) 457–468.
[23] J.R. Sanchez-Ramos, S. Song, S.G. Kamath, T. Zigova, A. Willing, F. Cardozo-Pelaez, T. Stedeford, M. Chopp, P.R. Sanberg, Expression of neural markers in human umbilical cord blood, Exp. Neurol. 171 (2001) 109–115.
[24] T. Kato, T. Heike, K. Okawa, M. Haruyama, K. Shiraishi, M. Yoshimoto, M. Nagato, M. Shibata, T. Kumada, Y. Yamanaka, H. Hattori, T. Nakahata, A neurosphere-derived factor, cystatin C, supports differentiation of ES cells into neural stem cells, Proc. Natl. Acad. Sci. U. S. A. 103 (2006) 6019–6024.
[25] S. Wakitani, T. Saito, A.I. Caplan, Myogenic cells derived from rat bone marrow mesenchymal stem cells exposed to 5-azacytidine, Muscle Nerve 18 (1995) 1417–1426.
[26] M. Kanatsu-Shinohara, K. Inoue, J. Lee, M. Yoshimoto, N. Ogonuki, H. Miki, S. Baba, T. Kato, Y. Kazuki, S. Toyokuni, M. Toyoshima, O. Niwa, M. Oshimura, T. Heike, T. Nakahata, F. Ishino, A. Ogura, T. Shinohara, Generation of pluripotent stem cells from neonatal mouse testis, Cell 119 (2004) 1001–1012.
[27] K. Umeda, T. Heike, M. Yoshimoto, M. Shiota, H. Suemori, H.Y. Luo, D.H. Chui, R. Torii, M. Shibuya, N. Nakatsuji, T. Nakahata, Development of primitive and definitive hematopoiesis from nonhuman primate embryonic stem cells in vitro, Development 131 (2004) 1869–1879.
[28] W.S. Pear, G.P. Nolan, M.L. Scott, D. Baltimore, Production of high-titer helper-free retroviruses by transient transfection, Proc. Natl. Acad. Sci. U. S. A. 90 (1993) 8392–8396.
[29] B. de Crombrugghe, V. Lefebvre, R.R. Behringer, W. Bi, S. Murakami, W. Huang, Transcriptional mechanisms of chondrocyte differentiation, Matrix Biol. 19 (2000) 389–394.
[30] T.X. O'Brien, K.J. Lee, K.R. Chien, Positional specification of ventricular myosin light chain 2 expression in the primitive murine heart tube, Proc. Natl. Acad. Sci. U. S. A. 90 (1993) 5157–5161.
[31] S.W. Kubalak, W.C. Miller-Hance, T.X. O'Brien, E. Dyson, K.R. Chien, Chamber specification of atrial myosin light chain-2 expression precedes septation during murine cardiogenesis, J. Biol. Chem. 269 (1994) 16961–16970.
[32] H. Niwa, Molecular mechanism to maintain stem cell renewal of ES cells, Cell Struct. Funct. 26 (2001) 137–148.
[33] E. Ben-Shushan, J.R. Thompson, L.J. Gudas, Y. Bergman, Rex-1, a gene encoding a transcription factor expressed in the early embryo, is regulated via Oct-3/4 and Oct-6 binding to an octamer site and a novel protein, Rox-1, binding to an adjacent site, Mol. Cell. Biol. 18 (1998) 1866–1878.
[34] A. Kispert, B. Koschorz, B.G. Herrmann, The T protein encoded by Brachyury is a tissue-specific transcription factor, EMBO J. 14 (1995) 4763–4772.
[35] P. Tontonoz, E. Hu, B.M. Spiegelman, Stimulation of adipogenesis in fibroblasts by PPAR gamma 2, a lipid-activated transcription factor, Cell 79 (1994) 1147–1156.
[36] P. Ducy, R. Zhang, V. Geoffroy, A.L. Ridall, G. Karsenty, Osf2/Cbfa1: a transcriptional activator of osteoblast differentiation, Cell 89 (1997) 747–754.
[37] V. Lefebvre, P. Li, B. de Crombrugghe, A new long form of Sox5 (L-Sox5), Sox6 and Sox9 are coexpressed in chondrogenesis and cooperatively activate the type II collagen gene, EMBO J. 17 (1998) 5718–5733.
[38] H.H. Arnold, B. Winter, Muscle differentiation: more complexity to the network of myogenic regulators, Curr. Opin. Genet. Dev. 8 (1998) 539–544.
[39] T.J. Lints, L.M. Parsons, L. Hartley, I. Lyons, R.P. Harvey, Nkx-2.5: a novel murine homeobox gene expressed in early heart progenitor cells and their myogenic descendants, Development 119 (1993) 419–431.
[40] U. Lendahl, L.B. Zimmerman, R.D. McKay, CNS stem cells express a new class of intermediate filament protein, Cell 60 (1990) 585–595.
[41] P. Tropel, N. Platet, J.C. Platel, D. Noel, M. Albrieux, A.L. Benabid, F. Berger, Functional neuronal differentiation of bone marrow-derived mesenchymal stem cells, Stem. Cells (2006).
[42] J. Sanchez-Ramos, S. Song, F. Cardozo-Pelaez, C. Hazzi, T. Stedeford, A. Willing, T.B. Freeman, S. Saporta, W. Janssen, N. Patel, D.R. Cooper, P.R. Sanberg, Adult bone marrow stromal cells differentiate into neural cells in vitro, Exp. Neurol. 164 (2000) 247–256.
[43] R.M. Seaberg, S.R. Smukler, T.J. Kieffer, G. Enikolopov, Z. Asghar, M.B. Wheeler, G. Korbutt, D. van der Kooy, Clonal identification of multipotent precursors from adult mouse pancreas that generate neural and pancreatic lineages, Nat. Biotechnol. 22 (2004) 1115–1124.
[44] F.M. Lamoury, J. Croitoru-Lamoury, B.J. Brew, Undifferentiated mouse mesenchymal stem cells spontaneously express neural and stem cell markers Oct-4 and Rex-1, Cytotherapy 8 (2006) 228–242.
[45] J. Deng, B.E. Petersen, D.A. Steindler, M.L. Jorgensen, E.D. Laywell, Mesenchymal stem cells spontaneously express neural proteins in culture and are neurogenic after transplantation, Stem. Cells 24 (2006) 1054–1064.
[46] A.R. Alexanian, Neural stem cells induce bone-marrow-derived mesenchymal stem cells to generate neural stem-like cells via juxtacrine and paracrine interactions, Exp. Cell Res. 310 (2005) 383–391.
[47] S. Wislet-Gendebien, P. Leprince, G. Moonen, B. Rogister, Regulation of neural markers nestin and GFAP expression by cultivated bone marrow stromal cells, J. Cell Sci. 116 (2003) 3295–3302.
[48] M. Baddoo, K. Hill, R. Wilkinson, D. Gaupp, C. Hughes, G.C. Kopen, D.G. Phinney, Characterization of mesenchymal stem cells isolated from murine bone marrow by negative selection, J. Cell. Biochem. 89 (2003) 1235–1249.
[49] D. Orlic, J. Kajstura, S. Chimenti, I. Jakoniuk, S.M. Anderson, B. Li, J. Pickel, R. McKay, B. Nadal-Ginard, D.M. Bodine, A. Leri, P. Anversa, Bone marrow cells regenerate infarcted myocardium, Nature 410 (2001) 701–705.
[50] K. Fukuda, Progress in myocardial regeneration and cell transplantation, Circ. J. 69 (2005) 1431–1446.
[51] H. Kawada, J. Fujita, K. Kinjo, Y. Matsuzaki, M. Tsuma, H. Miyatake, Y. Muguruma, K. Tsuboi, Y. Itabashi, Y. Ikeda, S. Ogawa, H. Okano, T. Hotta, K. Ando, K. Fukuda, Nonhematopoietic mesenchymal stem cells can be mobilized and differentiate into cardiomyocytes after myocardial infarction, Blood 104 (2004) 3581–3587.

[52] S. Tomita, D.A. Mickle, R.D. Weisel, Z.Q. Jia, L.C. Tumiati, Y. Allidina, P. Liu, R.K. Li, Improved heart function with myogenesis and angiogenesis after autologous porcine bone marrow stromal cell transplantation, J. Thorac. Cardiovasc. Surg. 123 (2002) 1132–1140.
[53] A.A. Mangi, N. Noiseux, D. Kong, H. He, M. Rezvani, J.S. Ingwall, V.J. Dzau, Mesenchymal stem cells modified with Akt prevent remodeling and restore performance of infarcted hearts, Nat. Med. 9 (2003) 1195–1201.
[54] H.F. Tse, Y.L. Kwong, J.K. Chan, G. Lo, C.L. Ho, C.P. Lau, Angiogenesis in ischaemic myocardium by intramyocardial autologous bone marrow mononuclear cell implantation, Lancet 361 (2003) 47–49.
[55] J.G. Shake, P.J. Gruber, W.A. Baumgartner, G. Senechal, J. Meyers, J.M. Redmond, M.F. Pittenger, B.J. Martin, Mesenchymal stem cell implantation in a swine myocardial infarct model: engraftment and functional effects, Ann. Thorac. Surg. 73 (2002) 1919–1925 (discussion 1926).

STEM CELLS®
EMBRYONIC STEM CELLS

# Sequential Analysis of α- and β-Globin Gene Expression During Erythropoietic Differentiation from Primate Embryonic Stem Cells

KATSUTSUGU UMEDA,[a] TOSHIO HEIKE,[a] MAMI NAKATA-HIZUME,[a] AKIRA NIWA,[a] MASATO ARAI,[a] GEN SHINODA,[a] FENG MA,[a] HIROFUMI SUEMORI,[b] HONG YUAN LUO,[c] DAVID H. K. CHUI,[c] RYUZO TORII,[d] MASABUMI SHIBUYA,[e] NORIO NAKATSUJI,[f] TATSUTOSHI NAKAHATA[a]

[a]Department of Pediatrics, Graduate School of Medicine, Kyoto University, Kyoto, Japan; [b]Laboratory of Embryonic Stem Cell Research, Stem Cell Research Center, Institute for Frontier Medical Sciences, Kyoto University, Kyoto, Japan; [c]Department of Medicine, Boston University School of Medicine, Boston, Massachusetts, USA; [d]Research Center for Animal Life Science, Shiga University of Medical Science, Ohtsu, Japan; [e]Division of Genetics, Institute of Medical Science, University of Tokyo, Tokyo, Japan; [f]Department of Development and Differentiation, Institute for Frontier Medical Science, Kyoto University, Kyoto, Japan

**Key Words.** Embryonic stem cells • Erythroid progenitors

ABSTRACT

**The temporal pattern of embryonic, fetal, and adult globin expression in the α (ζ → α) and β (ε → γ and γ → β) clusters were quantitatively analyzed at the transcriptional and translational levels in erythrocytes induced from primate embryonic stem cells in vitro. When vascular endothelial growth factor receptor-2$^{high}$ CD34$^{+}$ cells were harvested and reseeded onto OP9 stromal cells, two-wave erythropoiesis occurred sequentially. Immunostaining and real-time reverse transcription-polymerase chain reaction analyses of floating mature erythrocytes revealed that globin switches occurred in parallel with the erythropoietic transition. Colony-forming assays showed replacement of primitive clonogenic progenitor cells with definitive cells during culturing. A decline in embryonic ζ- and ε-globin expression at the translational level occurred in individual definitive erythroid progenitors. Expression of β-globin in individual definitive erythroid progenitors was upregulated in the presence of OP9 stromal cells. Thus, this system reproduces early hematopoietic development in vitro and can serve as a model for analyzing the mechanisms of the globin switch in humans.**
STEM CELLS *2006;24:2627–2636*

## INTRODUCTION

In all species, the shifting sites of erythropoiesis coincide with changes in the hemoglobin composition of erythrocytes. Primitive (embryonic) hematopoiesis initially occurs in the yolk sac, followed by definitive (fetal and adult) hematopoiesis, first in the aorta-gonad-mesonephros region and then in the fetal liver, spleen, and bone marrow [1, 2]. Concomitant switches in the α (ζ → α) and β (ε → γ and γ → β) clusters of erythrocytes occur during primate (human and monkey) development and coincide with a shift in the site of hematopoiesis. However, the regulatory mechanisms of globin switching in primates remain to be resolved, primarily due to the lack of available model systems that reproduce the process of hematopoiesis to reflect in vivo development accurately. Only limited in vitro studies of the switch from embryonic to fetal globin have been performed, due to restrictions on the use of primate embryos [3–5].

Recently, established primate embryonic stem cell (ESC) lines [6–9] have served as an experimental model for tissue growth and development, as an efficacy and toxicity screening system for new drugs, and as a cell source for regeneration therapy [10, 11]. Numerous reports also have demonstrated hematopoietic differentiation induced from primate ESCs in vitro [12–16]. We previously showed transition from primitive to definitive erythropoiesis in primate ESCs upon coculture with OP9 stromal cells [15]. Moreover, sequential fluorescence-activated cell sorting (FACS) analysis revealed that the vascular endothelial growth factor receptor-2 (VEGFR-2)$^{high}$ CD34$^{+}$

Correspondence: Tatsutoshi Nakahata, M.D., Ph.D., Department of Pediatrics, Graduate School of Medicine, Kyoto University, 54 Kawahara-cho, Shogoin, Sakyo-ku, Kyoto 606-8507 Japan. Telephone: 81-75-751-3290; Fax: 81-75-752-2361; e-mail: tnakaha@kuhp.kyoto-u.ac.jp Received April 7, 2006; accepted for publication July 26, 2006; first published online in STEM CELLS *EXPRESS* August 3, 2006.  1066-5099/2006/$20.00/0 doi: 10.1634/stemcells.2006-0199